PERFORMANCE OF HIGH STRENGTH CONCRETE ENCASED STEEL COMPOSITE COLUMNS

SASIKUMAR P* , MANJU R
Department of Civil Engineering, Kumaraguru College of Technology,Coimbatore-641049, Tamil Nadu, India.

This research investigated the axial compression behaviour of high strength concrete Encased Steel Composite (ESC) columns. Six high strength concrete ESC columns were made with M70 grade concrete, including with and without Alkaline Resistant Glass Fibre (AR-GF), all the specimens were tested after curing periods. A study of structural performance was conducted, which included axial load-deformation, ultimate load-carrying capacity, failure mode, ductility, and stiffness. As a result of the experiments, the failure mode of ESC columns without AR-GF are sudden failures once the peak load is reached, and with AR-GF at 1.20% volume prevented concrete covers from spalling and increased the load-carrying capacity. In the whole experimental study, the reinforcement ratio was maintained at a constant. In conclusion, the results of the experimental study were compared with the Finite Element (FE) model results, the FE model is help to prediction of axial compression behaviour of ESC columns.

Keywords: *Encased steel composite column, axial deformation, axial load, ductility, high strength concrete, stiffness*

1. Introduction

In the recent year High Strength Concrete (HSC) are used in high-rise buildings and the same encased composite steel columns are placed on the basement column of the building to increase the load-carrying capacity compared to the conventional concrete column. From the structural performance point of view encased composite steel columns are high stiffness, have excellent strength, and also reduce the ductility. The shear cracks are reduced compared to the conventional concrete column and also overall shear resistance is improved on encased composite steel column studied by [1]. Composite encased steel columns with HSC can have many benefits from a structural standpoint. Thus, research efforts have gradually shifted toward developing Concrete Encased Steel (CES) columns with HSC to increase strength and other properties are studied by [2-6]. Experimental research is involved in several works [2-9], numerical [7], and analytical CES columns with HSC have been investigated for their compressive behavior studied by [9-11]. Since the steel profile is completely covered by the concrete, the composite column is resistant to fire and corrosion. Based on a literature survey and previous research, the majority of works are conducted in normal strength concrete of encased composite steel column under the pure compression [12], uniaxial loading [13], biaxial loading [14], and cyclic loading studied by [15]. In recent years, high strength concrete is mostly used in bridges and basement columns with advanced concrete technology and is also available in various kinds of materials like admixtures of minerals and chemicals. To qualify for high-strength CES columns, the compression member must have a small element size and be durable by [16]. Tested the ten composite encased steel column inclusion of high strength concrete column 93 N/mm^2 and normal strength of steel under axial loading. The specimens are tested in concrete ESC columns with compressive strength of 94-104 N/mm^2 and yield strength of steel is 812-913 N/mm^2 [17]. For composite steel columns made of HSC, the load-bearing capacity is calculated using EN 1994-1-1. Using EN 1994-1-1 and AISC 360-16, measured the buckling resistance of ESC columns with concrete grade 90 N/mm^2 and high strength steel [18]. Previous research has shown that fibres used on high-strength concrete for concrete cover prevention are very beneficial [19]. This research work was done with six high strength concrete ESC columns tested under axial compression behaviour with and without AR-GF. Many research works were done with steel fibres on ESC columns, but AR-GF was studied up to mechanical properties level [20-22]. The transverse reinforcement spacing is mentioned in the different codes presented in Table 1 [23-27].

2.Experimental study

2.1.Material properties

The concrete used in the present study was designed of M70 grade in accordance with IS 10262. The 28-day compressive strength was 78.19 N/mm^2 without Alkaline Resistant Glass Fibre (AR-GF) and 82.60 N/mm^2 with AR-GF was achieved. Six high strength concrete ESC column specimens were studied in this work, such as ESC columns with and without 1.20% AR-GF volume. A straight fibre with a diameter of 14 microns and a length of 12mm was

*Autor corespondent/*Corresponding author*,
E-mail: sasiserene@gmail.com

Table 1

Tranverse reinforcement spacing as per current code design

Design code	Spacing of transverse reinforcement	Maximum spacing
IS 456: 2000	1.16 times main rebar; 2. 48 times diameter of transverse rebar; 3. 300 mm.	300 mm
EN 1994-1-1: 2004	Allowable spacing in maximum: 1. 20 times longitudinal rebar; 2. The smallest column dimensions; 3. 400 mm.	240 mm
AISC 360: 2016	Maximum ties must be spaced no closer than 0.5 times the minimum column dimension.	120 mm
ACI 318: 2008	Maximum spacing of transverse: 1. 16 times of longitudinal rebar diameter; 2. 48 times of transverse rebar 3. Least dimension of the column.	240 mm
JGJ 138-2016	It is not permissible to space transverse rebars more than 15 times the main rebar diameter.	195 mm

Fig. 1 - Alkaline Resistant Glass Fibre (AR-GF)

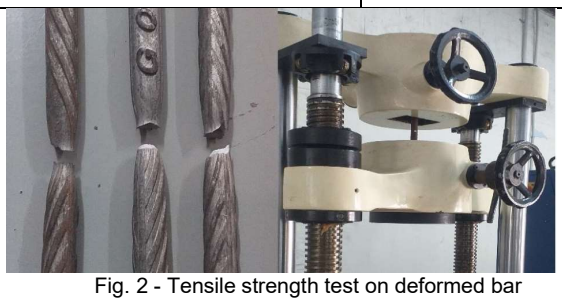

Fig. 2 - Tensile strength test on deformed bar

Table 2

Mix proportions

Specimen ID	% of AR-GF	C (kg)	FAS (kg)	SF (kg)	FA (kg)	CA (kg)	W (kg)	SP (kg)	W/B ratio
HSC1	0	419.20	52.40	52.40	595	1228	138	6.29	0.26
HSC2	1.20%	419.20	52.40	52.40	595	1228	138	6.29	0.26

Note-CE: Cement; FAS: Fly ash; SF: Silica fume; FA: Fine aggregate; CA: Coarse aggregate; W: Water; SP: Superplasticizer

Table 3

Properties of deformed bar

Sample	Diameter (mm)	Experimental study						
		P_y (kN)	σ_y (N/mm^2)	$\sigma_{y\,(avge)}$ (N/mm^2)	P_u (kN)	σ_u (N/mm^2)	$\sigma_{u\,(avge)}$ (N/mm^2)	E (N/mm^2)
1	12	37.28	329.56	339.73	51.02	451.15	464.08	2.05×10^5
2	12	39.24	346.98		53.46	472.72		1.98×10^5
3	12	38.95	342.65		52.97	468.38		1.97×10^5

Note-P_y and P_u: are referred to as yield and ultimate load; σ_y and σ_u: is refer as yield and ultimate stress; $\sigma_{y\,(avge)}$ and $\sigma_{u\,(avge)}$: is referred as yield and ultimate average stress; E: is referred as young's modulus

used in this present work and it is presented in Fig. 1. Table 2 provides the details on the concrete compositions and mixture proportions of AR-GF.

In this experiment, longitudinal and transverse reinforcement were provided by deformed steel bars 12 mm and 8 mm. Three samples of the steel bar are tested under the tensile test is shown in Fig. 2 and to be obtained the mechanical properties of yield strength, ultimate strength, breaking strength, and youngs modulus. The mechanical properties of reinforced bars were given in Table 3.

2.2.Preparation of specimens

The ESC specimens dimension details presented in Fig. 3. The ESC columns were prepared in a steel mould and the specimen preparation details were given in Fig. 4. Inside of the steel mould was lubricated with oil to prevent the concrete from adhering to the steel mould.

The reinforcement steel cage and I section was placed on the steel mould and positioned so that the pre-determined cover was available on all sides. The designed concrete mix was poured into the mould layer by layer and compacted with a tamping rod to avoid any honeycomb. According to the current standard, the spacing of internal tieswas provided as 100mm c/c throughout the column. The I section was placed on the inside of the reinforcement cage with the center to carry the load entire the column. Column dimensions are 150mm x 150mm x 1000mm, longitudinal reinforcement four numbers of 12 mm diameter bar and 8 mm diameter of transverse reinforcement are used, the grade is Fe 500 and mild steel Fe 250 of ISMB 100x50mm was used to make ESC columns. The geometry properties are summarized in Table 4. The specimens were removed from the steel mould without damage, kept for curing until 28 days.

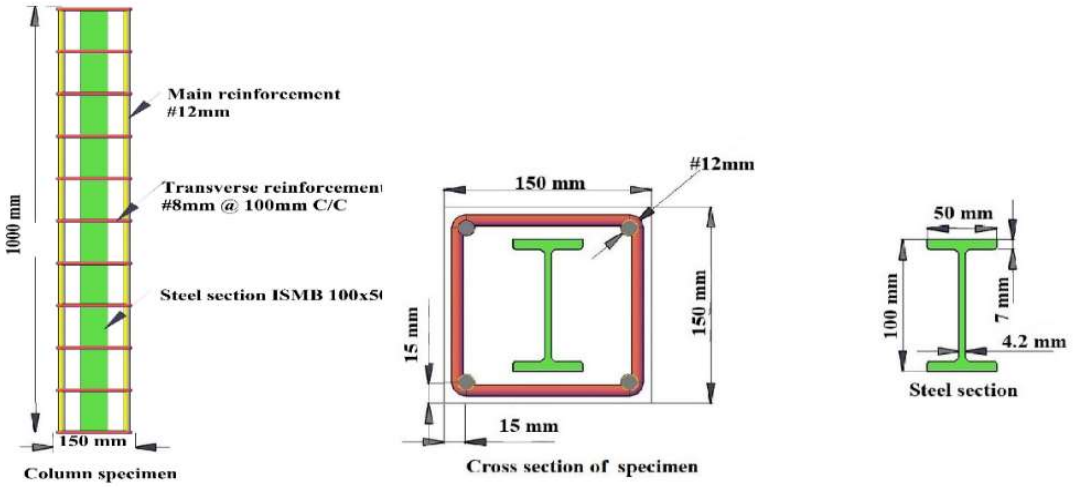

Fig. 3 - Dimension details of column specimen

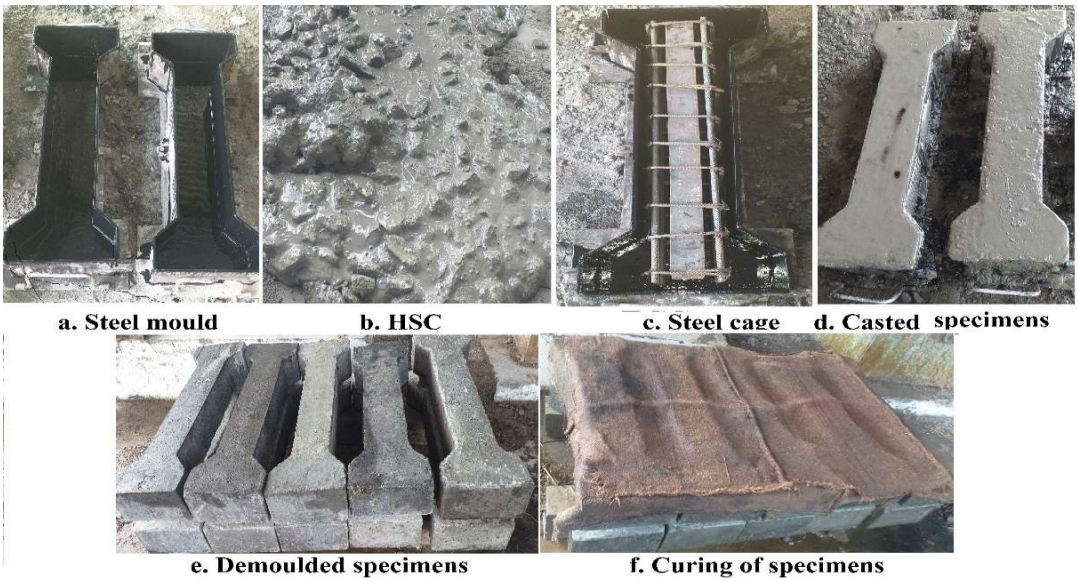

Fig. 4 - Encased steel composite column specimens

Table 4

Geometry properties of column specimens

ID	Specimen (mm)			Steel section (mm)				Reinforcement	
	B	D	L	t_f	t_w	B	D	Longitudinal bar	Tie bar
HSC1-1	150	150	1000	7	4.2	50	100	4 No. #12mm	#8mm@100mmc/c
HSC1-2	150	150	1000	7	4.2	50	100	4 No. #12mm	#8mm@100mmc/c
HSC1-3	150	150	1000	7	4.2	50	100	4 No. #12mm	#8mm@100mmc/c
HSC2-1	150	150	1000	7	4.2	50	100	4 No. #12mm	#8mm@100mmc/c
HSC2-2	150	150	1000	7	4.2	50	100	4 No. #12mm	#8mm@100mmc/c
HSC2-3	150	150	1000	7	4.2	50	100	4 No. #12mm	#8mm@100mmc/c

2.3.Specimen test

Testing was performed in a 200 T capacity loading frame, all the specimens were tested until collapse load. The specimens are placed axially with proper alignment in the loading frame. Three linear variable displacement transducers (LVDTs) were placed, one was placed vertical direction, and the remaining two are placed in the lateral direction of the specimen. During the testing period, the specimen was tested under the axial loading as shown in Fig. 5.

3.Analytical study

3.1.Finite Element (FE) modeling

An axial compression model for ESC columns was developed in a nonlinear 3D finite element Programme. FE modeling incorporated geometric and material nonlinearities to predict the behavior of a system.

3.2.Approach of the overall model

The ESC columns are considered three parts as shown in Fig. 6. Even though axial compression load persists within the cross-section,

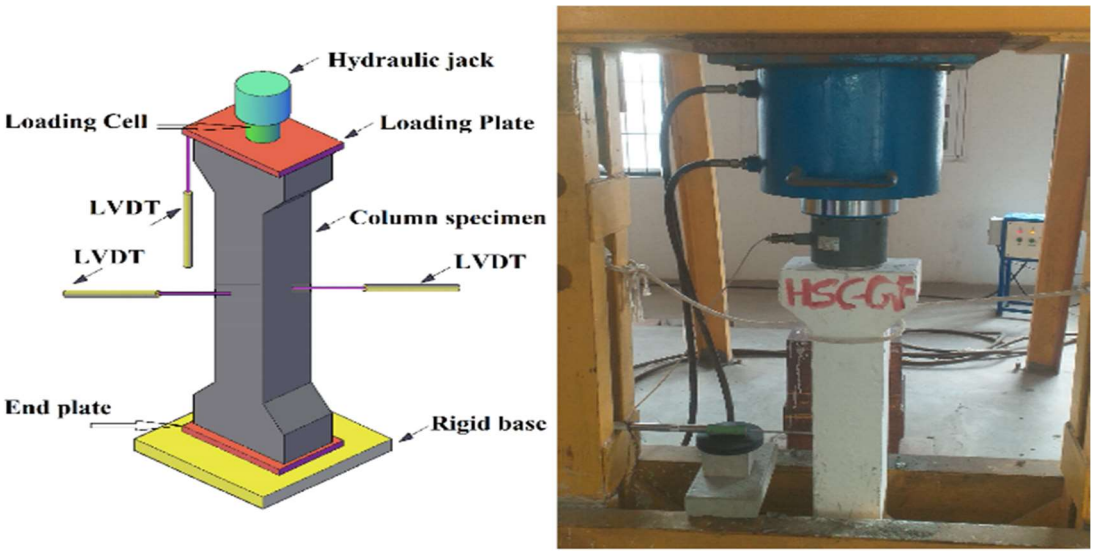

Fig. 5 - Test setup and instrumentation of column specimen

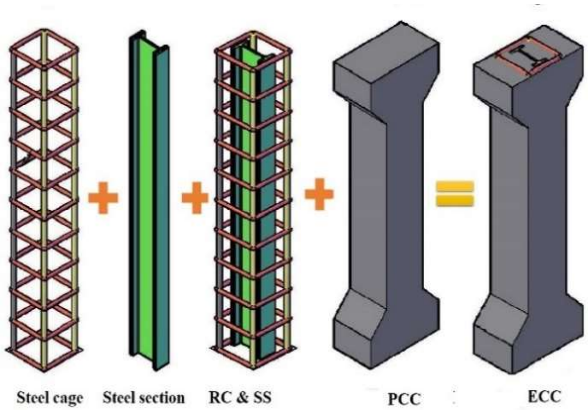

Fig. 6 - Encased steel composite column

The total concrete area of an HSC was considered, reinforcement, and steel section for model convenience

In non-linear problems that involve deformable bodies in contact with each other and plasticity with excessive distortion, ESC column specimens offer three degrees of freedom for translation. Based on the rigid body model, the top-loading plate was modeled using reference points that were not considered when analyzing it. ESC columns were constructed by using different components, including reinforcement cage, steel sections, and high strength PCC. For simulating the finite element model, a static general solution strategy was adopted.

3.3. Mesh convergence study

To minimize the computational cost, the mesh size was carefully selected to reduce the accuracy of the analysis without compromising efficiency. For encased composite columns, varying mesh sizes were tested. Large nominal mesh sizes were preferred despite coarse mesh sizes giving good results and being computationally less expensive since small nominal mesh sizes didn't accurately represent failure modes and did not allow smooth axial load and deformation responses around contours. The modeling of mesh was presented in Fig. 7.

3.4.Support conditions

In the analysis, displacement of the rigid body of the column specimens was controlled to apply axial load. As the axial loads were applied in the column and plates of steel measuring 10 mm thick were placed at each end. In the support condition, the top is pinned, while the bottom is fixed. The load-deformation behaviour of the column was not significantly affected by end conditions as shown in Fig. 8. To reproduce the displacement constraints applied during the tests, the top support of the column was restrained in translational degrees of freedom as well as in axial degrees of freedom. Because of the permanent attachment of the thick steel plate at the bottom of the bottom support and the absence of slip between the columns, the degree of freedom of translation was fixed.

3.5.Test results are verified using the finite element model

Results of experimental testing are summarized in Table 4 based on the validated FE model. A six columns array of ESC of 150 mm x 150 mm

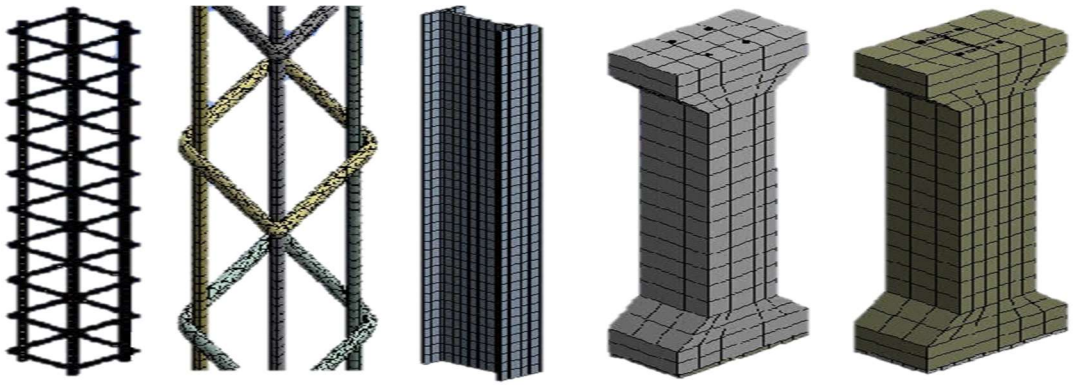

Fig. 7 - Meshing of ESC column in the finite element model

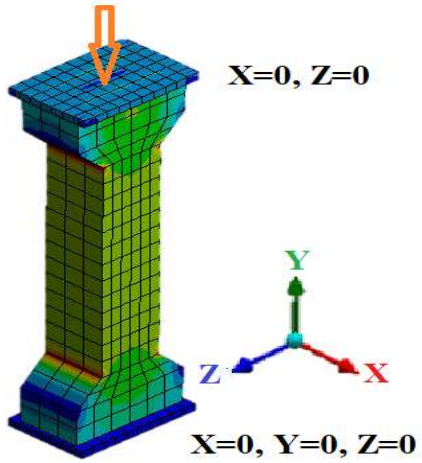

Fig. 8 - Axial load in finite element model

Table 5

Comparison of experimental and analytical results

ID	Experimental load (kN)	Stress (N/mm^2)	Average stress (N/mm^2)	Analytical load (kN)	Stress (N/mm^2)	Average stress (N/mm^2)
HSC1-1	1172	52.09	52.10	1181	52.49	52.79
HSC1-2	1165	51.78		1189	52.84	
HSC1-3	1180	52.44		1193	53.02	
HSC2-1	1276	56.71	56.73	1294	57.51	57.50
HSC2-2	1264	56.18		1288	57.24	
HSC2-3	1289	57.29		1299	57.73	

was tested under axial loading and categorized into two groups depending on whether the AR-GF was present. The first group is included ESC columns without AR-GF (HSC1). The second group of ESC with AR-GF (HSC2). Test parameters of two-column groups were studied including material strengths, and axial behaviour. Table 5 compares the test results of columns with the experimental results on the behaviour of axial compression.

3.6.Axial load-deformation response

Experimental and analytical results on axial load-deformation response is compared for all HSC1 – HSC2 is shown in Figs. 9-11, and axial stress response are presented in Fig. 12. It shows that FE models gave good predictions on peak loads, deformation, and mode of failure that corresponded well with test results. As much as 70 % of peak load was linearly responded to by all ESC columns, with a sudden drop in a stable residual strength was observed post-peak load. Compared HSC1 to HSC2 the strength decline was greater and more abrupt, reflecting the more brittle failure of the material. Based on the analytical analysis and experimental results, Table 6 compares peak-load and deformation calculated for all columns. From the present work its shows that, the analytical model provides a reliable prediction on ultimate strength of ESC columns. Similarly, peak-deformation predictions were well within ±7% of tested values, though some differences were seen from experimental results. With a standard deviation of 0.01 and a mean ratio of 0.99, the users achieved a good result.

4. Results and discussion

4.1.The Axial Load Carrying (ALC) capacity according to the standard code provisions

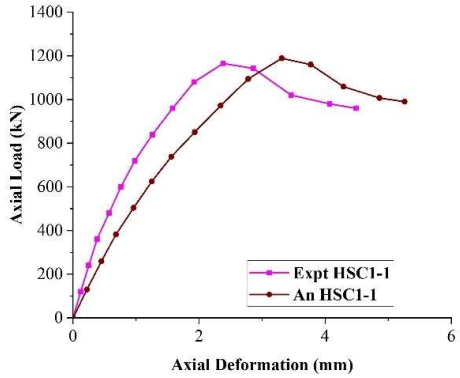

a. HSC1-1

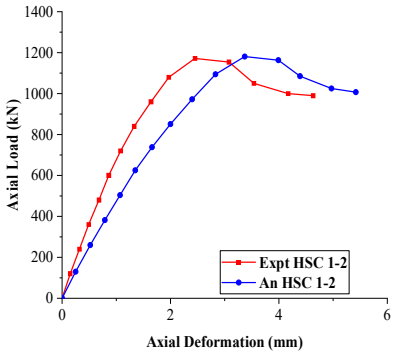

b. HSC1-2

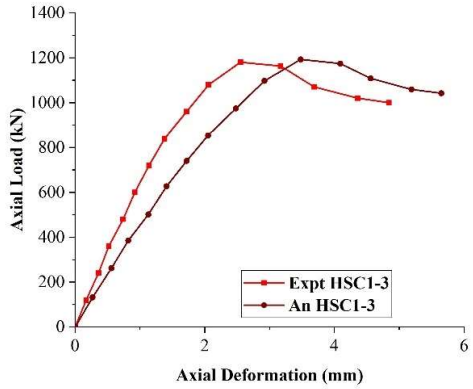

c. HSC1-3

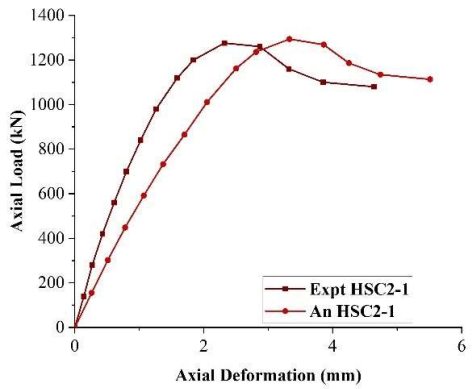

d. HSC2-1

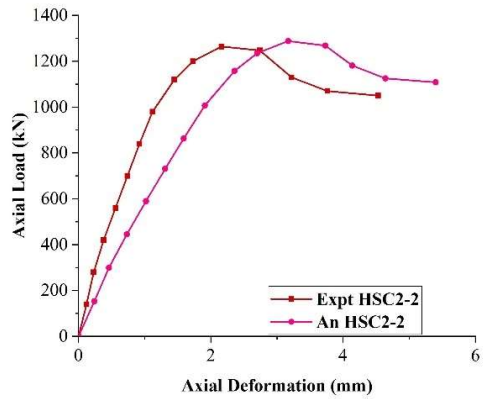

e. HSC2-2

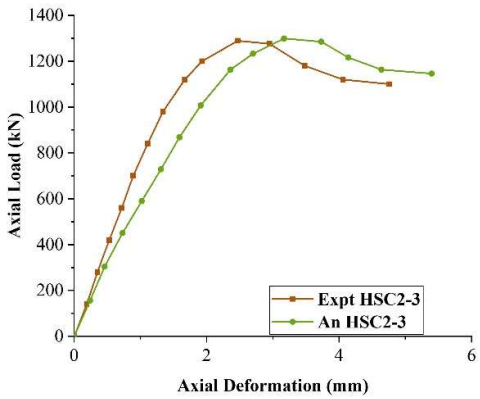

f. HSC2-3

Fig. 9 - Effect axial load-deformation in experimental response for column groups of HSC 1- 2

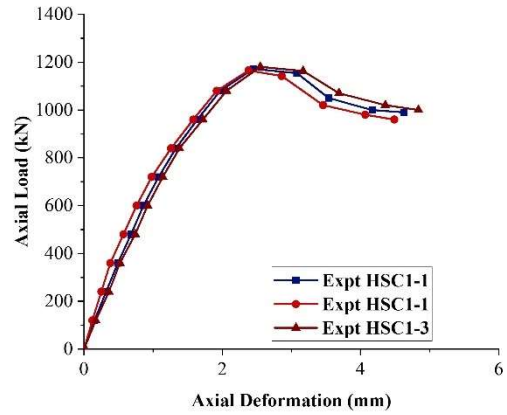

a. HSC1

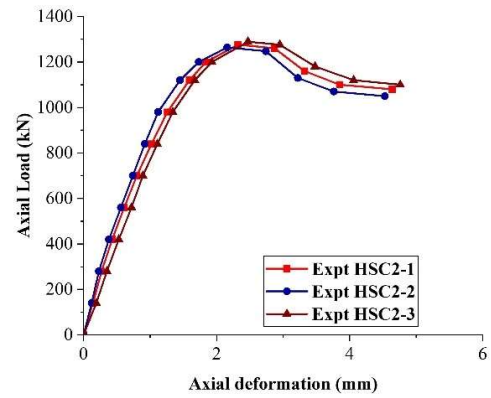

b. HSC2

Fig 10 - Effect axial load-deformation in experimental response for column groups of HSC 1-2

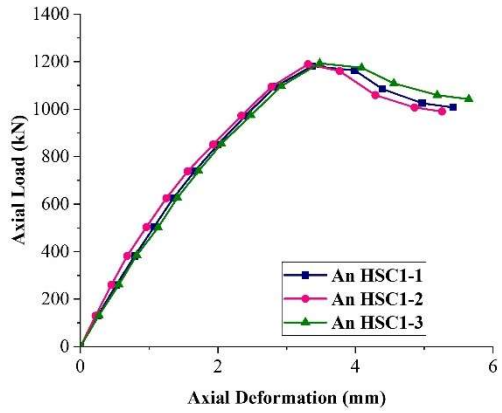

a. HSC1

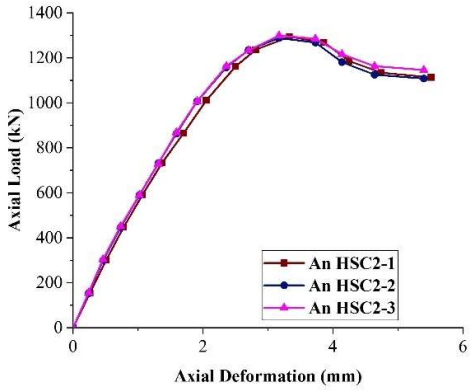

b. HSC2

Fig. 11 - Effect axial load-deformation in analytical response for column groups of HSC1- 2

Table 6

Test results of the ultimate axial load compared with analytical results

ID	Design load (kN)	Experimental load (kN)	Analytical load (kN)	P_{expt} / P_{an}	P_{design} / P_{expt}
HSC1-1	1104	1172	1181	0.99	0.94
HSC1-2	1104	1165	1189	0.98	0.95
HSC1-3	1104	1180	1193	0.99	0.94
HSC2-1	1143	1276	1294	0.99	0.90
HSC2-2	1143	1264	1288	0.98	0.90
HSC2-3	1143	1289	1299	0.99	0.89
Mean		-	-	0.99	0.93
Standard deviation		-	-	0.01	0.02

Based on the previous study, the ALC capacity of ESC columns is calculated by the Eqs. (1) and (2) by [18].

$$\text{Euro code } N = 0.85A_c f_c + A_s f_{ys} + A_r f_{yr} \quad (1)$$

$$\text{China code } N = 0.90(A_c f_c + A_s f_{ys} + A_r f_{yr}) \quad (2)$$

Where, A_c. A_s and A_r are referred to as area of concrete, area of steel section, and area of longitudinal reinforcement of bar respectively. f_c, $f_{ys,}$ and f_{yr} refer to the compressive strength of concrete, yield strength of steel section, and yield strength of longitudinal reinforcement bar respectively.

Composite column construction is not specifically mentioned in the Indian standard IS: 11384-1985. The composite column design provision is contained from IS: 456 – 2000. Composite column Eq (3) will be extended as following results.

$$\text{Indian code } P_P = A_a P_y + A_c P_{ck} + A_s P_{sk} \quad (3)$$

Where:

$P_y = 0.87f_{y;}$

$P_{ck} = 0.4\ (f_{ck})_{cu}$ and

$P_{sk} = 0.67f_y$

In Indian standard code where A_a, $A_{c,}$ and A_s are refer to the area of concrete, area of steel section, and area of longitudinal reinforcement of bar respectively. P_y, P_{ck} and P_{sk} are referring to the compressive strength of concrete, yield strength of steel section, and yield strength of longitudinal reinforcement bar respectively.

4.2. Comparison between axial load-deformation response in experimental and analytical results

The ESC column specimens are tested under axial loading. The axial load verse deformation shortening curve for initial stage of the specimen is linear behaviour, and the high strength concrete column with AR-GF is more stiffener compared to the without AR-GF column specimens HSC1, and HSC2 are shown in Fig. 13. The maximum ALC capacity and axial deformation of the ESC columns are presented in Fig. 14. The details of peak load are mentioned in Table 5. total of 6 column specimens are tested under the axial load, the ALC capacity is more compared to the without AR-GF column specimens.

A load-deformation curve shows that the axial load reaches the elastic to the plastic phase when reaching 70 % of ultimate ALC capacity and resulting stiffness of the HSC column with AR-GF may be considered excellent, after reaching the specimen in ultimate load, the axial load is gradually decreased, and the specimen is failed suddenly with cover spalling. The HSC1 with AR-GF specimens are failed without cover spalling and the minor only formed when reached peak load.

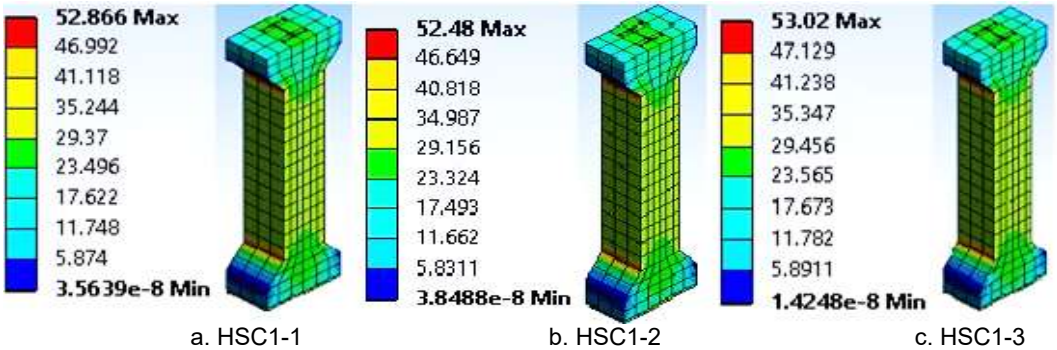

a. HSC1-1 b. HSC1-2 c. HSC1-3

d. HSC2-1 e. HSC2-2 f. HSC2-3

Fig. 12 - Stress distribution for column groups HSC1&2

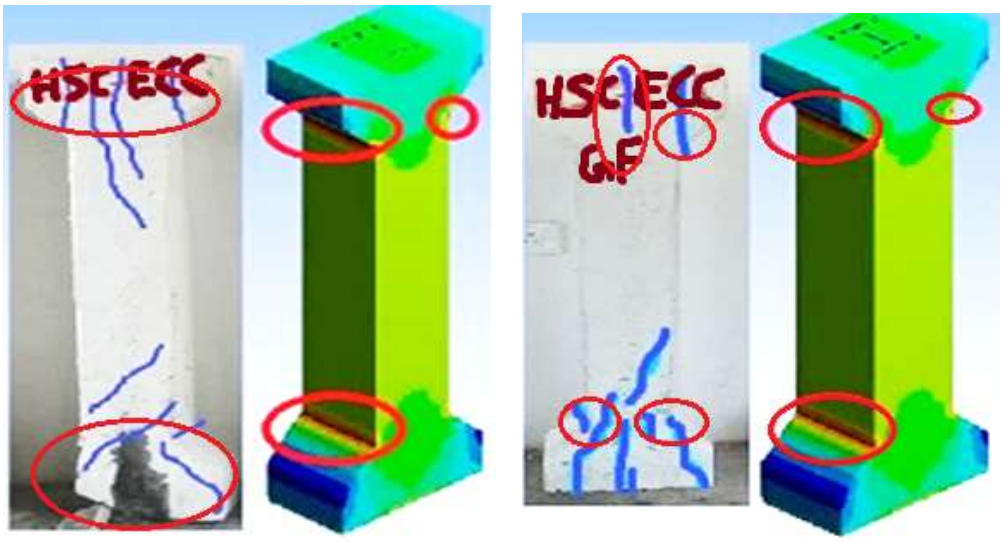

a. HSC 1 b. HSC 2

Fig. 13 - Comparison between experimental and analytical behaviour of column group of HSC1&2

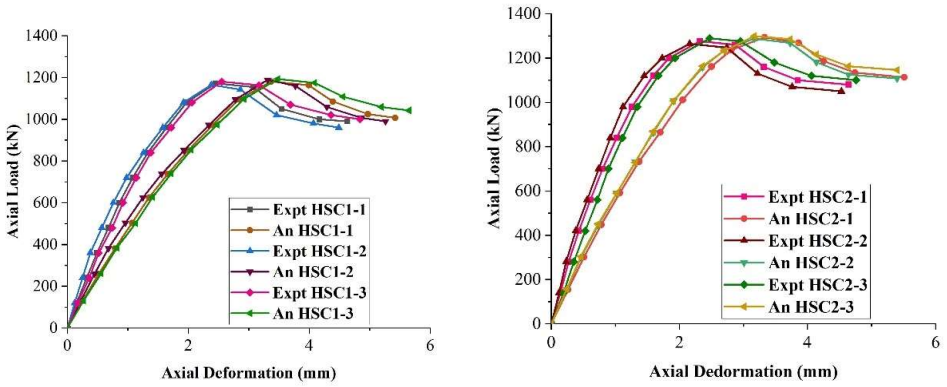

a. HSC 1 b. HSC 2

Fig. 14- Experimental and analytical axial load-deformation response in column groups of HSC 1&2

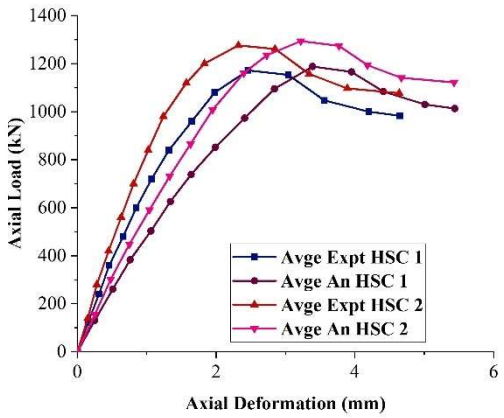

Fig. 15 - Average experimental and analytical axial load-deformation response in all columns

ultimate load is failed without concrete cover spalling and crack. after reaching the ultimate load, the load is increased gradually in certain intervals the crack in initiate is the longitudinal direction in the bottom and top region of the column specimens.

4.4. Concrete strength affects structural performance

The concrete strength is increased with the addition of AR-GF on high-strength concrete. The axial load carrying capacity is increased on ESC column 1172 kN to 1276 kN respectively. The average axial load carrying capacity is presented in Fig. 15. lower ductility is presented without AR-GF specimens, and sudden failure pattern, more major crack and cover spalling are presented.

a. HSC1 b. HSC2

Fig.16 - The failure mode of specimens

Table 7

Experimental results and mode of failure

ID	Experimental load (kN)	Stress (N/mm^2)	Average stress (N/mm^2)	Mode of failure
HSC1-1	1172	52.09	52.10	CS + CC
HSC1-2	1165	51.78		CS + CC + CSP
HSC1-3	1180	52.44		CS + CC
HSC2-1	1276	56.71	56.73	CC + FP
HSC2-2	1264	56.18		CC
HSC2-3	1289	57.29		CC + FP

Note-CS: Cover spalling; CC: Concrete crushing; CSP: Concrete splitting; FP: Fibre pullout

4.3. Failure mode

Fig. 16 shows the specimens after they have been tested under axial loading. Different failure modes are observed from all tested specimens in this study is summarized in Table 7. The common observation in all specimens is failed in crushing mode. But the inclusion of 1.20% AR-GF is prevented the concrete cover from spalling and increases structural performances of ESC columns. The minor cracks were formed before reaching the ultimate load without AR-GF in both ESC columns, same as few specimens are failure with a loud sound to continuously axial load applying after reaching peak load. Meanwhile, with the addition of AR-GF, both ESC columns are reaches maximum

4.5. Effect of alkaline resistant glass fibre

Alkaline resistant glass fibre reinforced concrete encased steel composite concrete strength is presented during the tested period the performance is excellent compared to the without AR-GR specimens. Addition 1.20% of AR-GF is increasing load-carrying capacity and prevented the cover spalling when the specimens are leading attained the maximum ultimate load. The axial load carrying capacity is increased encased steel composite column is 8.87% compared to the without AR-GF, the spacing of transverse reinforcement 100mm c/c. Based on the experimental and observation from the tested encased steel composite column specimens are

Table 8

Experimental structural behaviour of the high strength concrete specimens

ID	Yield point			Ultimate point			$D_{0.75}$ (mm)	m	Ultimate Stiffness (K) kN/mm
	Py (kN)	D_y (mm)	ε_y	P_u (kN)	D_u (mm)	ε_u			
HSC1-1	830	1.33	0.00133	1172	2.45	0.00245	3.08	2.31	478.37
HSC1-2	850	1.26	0.00126	1165	2.38	0.00238	2.86	2.26	489.50
HSC1-3	840	1.38	0.00138	1180	2.55	0.00255	3.17	2.29	462.75
HSC2-1	980	1.26	0.00126	1276	2.32	0.00232	2.87	2.27	550.00
HSC2-2	960	1.12	0.00112	1264	2.16	0.00216	2.74	2.44	585.19
HSC2-3	985	1.34	0.00134	1289	2.47	0.00247	2.95	2.20	521.86

Note-P_y and P_u: is denoted as yield and ultimate axial load; D_y and D_u: is denoted as yield and ultimate deformation; Ɛy and Ɛu: is refer yield and ultimate strain; m: refer as ductility index

indicating the AR-GF is increasing the axial load carrying capacity, preventing the concrete cover spalling, improvement of strength, and ductility.

4.6. Post peak ductility

The ductility is more important in reinforced concrete members for seismic design. In Hadi et al. [28] mention the ductility index and they calculation of the ductility index involves formulating Eq (4) as the ratio between the axial deformation as a result of 75% of the maximum axial load and the axial deformation as a result of yielding the axial deformation.

$$\mu = \frac{\mathrm{D0.75}}{\mathrm{Dy}} \tag{4}$$

Table 8 provides a calculation of ductility index m. When the longitudinal reinforcement bar is compressed axially, the yield point occurs in the steel section. The conventional HSC1 columns have high ductility compared to the inclusion of AR-GF specimens. Tie spacing is more important to increase load-carrying capacity, prevented the concrete cover spalling, and ductility in ESC columns. Finally conclude that the 1.20% AR-GF is more sufficient to reduce the ductility compared with reducing the transverse reinforcement spacing.

5. Conclusion and recommended future work

In this paper, we study experimentally and analytically the axial performance of ESC columns. In this study, the effects of axial load carrying capacity, axial deformation response, failure mode, and behavior of alkaline-resistant glass fiber were considered. Also studied in ductility, stiffness of the ESC column. Analysis of the experimental results enabled the prediction of experimental results by using the analytical results. The following conclusion is reported in this paper:

- The experimental results were investigated in ESC columns made with HSC inclusion of with and without alkaline resistant glass fibre.
- According to the experimental results, the ESC columns longitudinal reinforcement bar, steel section reaches the yield strength before attaining the ultimate load.
- The test specimens of ESC column without AR-GF where concrete cover spalling is increasing poor ductility after reaching peak load, same as with AR-GF specimens cover spalling is smoothly increased ductility after reaching the peak load.
- The tested specimens of ESC columns without AR-GF, after reaching the yield load the specimens is failure gradually with sudden crack and concrete cover spalling is increasing poor ductility after reaching peak load, same as with AR-GF the specimens were failed with the minor crack when the specimen reaches the peak load without cover spalling.
- The effect of the ALC capacity by concrete cover spalling ESC columns. Mainly axial load capacity is affected by later reinforcement spacing, it was necessary to increase peak load to reduce the spacing between transverse reinforcements ESC of column specimens.
- The AR-GF ESC columns are shown good structural performance compared to the without AR-GF. With 1.20% AR-GF, a concrete cover not spall and also have improved load carrying capacity, reduced ductility, and increased stiffness.
- FE model analysis was more efficient to predict the peak axial load of both ESC columns under compression behaviour.

Future research will be considered on the structural performance of the ESC column made with HSC with HS steel with different spacing of transverse reinforcement. The alkaline resistant glass fibre and steel fibre are further investigated. In addition, the structural behaviour of ESC specimens will be studied under different loading conditions.

REFERENCES

[1] M. Zhu, J. Liu, Q. Wang and X. Feng, Experimental research on square steel tubular columns filled with steel reinforced self-consolidating high-strength concrete under axial load, Eng. Struct., 2010, **32**(8), 2278–2286.

[2] C.S. Kim, H.G. Park, K.S. Chung and I.R. Choi, Eccentric axial load testing for concrete-encased steel columns using 800 MPa steel and 100 MPa concrete, J. Struct. Eng., 2011, **138**(8), 1019–1031.

[3] B. Lai, J.R. Liew and H.A. Le, Behavior of high strength concrete encased steel composite stub columns with C130 concrete and S690 steel, Eng. Struct., 2019, **200**,109743.
[4] B. Lai, J.R. Liew and M. Xiong, Experimental study on high strength concrete encased steel composite short columns. Constr. Build. Mater., 2019, **228**, 116640.
[5] B. Lai, J.R. Liew, A. Venkateshwaran, S. Li and M. Xiong, Assessment of high-strength concrete encased steel composite columns subject to axial compression, J. Constr. Steel. Res., 2020, **164**, 105765.
[6] M. Begum, R.G. Driver and A.E. Elwi, Behaviour of partially encased composite columns with high strength concrete, Eng. Struct., 2013, **56**, 1718–1727.
[7] E. Ellobody and B. Young, Numerical simulation of concrete encased steel composite columns, J. Constr. Steel Res., 2011, **67**, 211–222.
[8] W.Q. Zhu, G. Meng and J.Q. Jia, Experimental studies on axial load performance of high-strength concrete short columns, Proc. Inst. Civ. Eng. Struct. Build., 2014, **167**(9), 509–519.
[9] B. Lai, J.Y. Liew and M. Xiong, Experimental and analytical investigation of composite columns made of high strength steel and high strength concrete, Steel Compos. Struct., 2019, **33**(1), 899–911.
[10] S. Chen and P. Wu, Analytical model for predicting axial compressive behavior of steel reinforced concrete column, J. Constr. Steel Res., 2017, **128**, 649–660.
[11] C.C. Chen and N.J. Lin, Analytical model for predicting axial capacity and behavior of concrete encased steel composite stub columns, J. Constr. Steel Res., 2006, **62**(5), 424–433.
[12] Y. Liu, Z.X. Guo, P.H. Xu and L.P. Jia, Experimental study on axial compression behavior of core steel reinforced concrete columns, J. Build. Struct., 2015, **36**(4), 68–74.
[13] G.T. Zhao, C.H. Wang, C.Y. Gao and Wang, Experiment study on the capacity of SRC long column subjected to eccentric compression, J. Baotou Univ. Iron Steel Technol., 2006, **4**, 384–400.
[14] C. Dundar, S. Tokgoz, A.K. Tanrikulu and T. Baran, Behaviour of reinforced and concrete-encased composite columns subjected to biaxial bending and axial load, Build. Environ., 2008, **43**(6), 1109–1120.
[15] C. Campian, Z. Nagy and M. Pop, Behavior of fully encased steel-concrete composite columns subjected to monotonic and cyclic loading, Proc. Eng., 2015, **117**, 439–451.
[16] H.A. Le and E. Fehling, Influence of steel fiber content and aspect ratio on the uniaxial tensile and compressive behavior of ultra-high-performance concrete, Constr. Build. Mater., 2015, **153**, 790–806.
[17] C.S. Kim, H.G. Park, K.S. Chung and I.R. Choi, Eccentric axial load capacity of high- strength steel-concrete composite columns of various sectional shapes, J. Struct. Eng., 2013, **140**, 04013091.
[18] B.L. Lai, J.Y.R. Liew and T.Y. Wang, Buckling behaviour of high strength concrete encased steel composite columns, J. Constr. Steel Res., 2019d, **154**, 27–42.
[19] C.C. Hung and F.Y. Hu, Behavior of high-strength concrete slender columns strengthened with steel fibers under concentric axial loading, Constr. Build. Mater., 2018, **175**, 422–433.
[20] M.M. Hilles, M. Mohammed and Ziara, Mechanical behavior of high strength concrete reinforced with glass fiber, Eng. Science Technol. International J., 2019, **22**, 920–928.
[21] Z. Shi, Q. Wang and L. Xu, Experimental Study of Cement Alkali-Resistant Glass Fiber (C-ARGF) Grouting Material. Mater., 2020,**13**, 605.
[22] Z.D. Zhu, Z. D., C. Zhang, S.S. Meng, S.Z. Tao and D. Zhu, A statistical damage constitutive model based on the Weibull distribution for alkali-resistant glass fiber-reinforced concrete, Mater., 2019, **12**, 1908
[23] IS 456 {2000), plain and reinforcement concrete – code of practice. Indian standard.
[24] EN 1994-1-1. (2004), Eurocode 4: Design of Composite Steel and Concrete Structures- Part 1-1. General Rules and Rules for Buildings. Euro code.
[25] AISC 360 (2016), Specification for Structural Steel Buildings. Chicago: American Institute of Steel Construction.
[26] ACI 318 (2008), Building Code Requirement for Structural Concrete and Commentary. American Concrete Institute.
[27] JGJ 138 (2016), Code for design of composite structures. China: Ministry of Housing and Urban-Rural Development of the People's Republic of China.
[28] M.N. Hadi, A.A. Ibrahim and M.N. Sheikh, Behavior of high-strength concrete columns reinforced with galvanized steel equal-angle sections under different loading conditions, J. Struct. Eng., 2011, **144**(7), 04018070.

****